Comparisons between numerical and experimental data for the planar rocking-block dynamics – Part II: analysis of the onset of rocking and of overturning

Hongjian Zhang*, Bernard Brogliato†, Caishan Liu‡

May 16, 2011

Abstract

In this Part II it is considered that the base has a horizontal motion. The parameters that have been fitted with free-rocking experiments in Part I are used to study the onset of rocking and the onset of overturning. Very good agreement with experimental data, when they exist, are found. Some new ideas on possible criteria for onset of rocking and overturning are provided from the extensive numerical results.

Keywords: rocking block, multiple impacts, Coulomb friction, overturning.

1 Introduction

Studying the onset of rocking and the onset of overturning of blocks is of great interest in the Earthquake Engineering literature in order to improve the safety of buildings, furnitures *etc* under seismic motions. Let us mention [1, 3, 10, 12, 13, 14, 15, 21, 22, 26, 28, 30, 32, 34, 36] to cite a few of the published works on this topic. Several different modeling approaches have been tried in the literature and many experimental tests have been led on various types of systems (ranging from granite blocks of several hundred kg [24], wood blocks of several hundred grams [3], to real-life fridges or furnitures [13]). Also various types of base excitations have been considered: harmonic [1, 8, 10, 12, 34], one-sine pulse [22, 30, 36], random [28], extracted from real earthquakes measurements [1, 13, 26, 32, 34]. The aim of these works is essentially at determining conditions such that a structure subject to base excitation (horizontal, vertical or both) may start to rock, or may overturn. A major conclusion that is drawn from many of these works is that the classical Housner approach [11] for modeling the block/ground dynamics is too limited and cannot correctly model the rich dynamics of such nonsmooth nonlinear systems [9, 21, 24]. This is mainly due to the fact that the Housner basic assumptions of perfect sticking of the contact/impact points (in both the normal and the tangential directions) is usually not satisfied: rebounds and stick/slip motions exist in most of the cases. This is already true for fixed-base free-rocking motions (except if the block is slender enough, the friction is large enough and the normal restitution dissipates enough energy), and becomes even more crucial when the base is moving. For these reasons other models have been used: DEM [23, 24, 34], linearized models of rocking [1, 36], improved Housner with

*State Key Laboratory for Turbulence and Complex Systems, College of Engineering, Peking University, Beijing 100871, People's Republic of China. Work performed while at INRIA, BIPOP project-team, ZIRST Montbonnot, 655 avenue de l'Europe, 38334 Saint Ismier, France, e-mail: hongjian.zhang@inrialpes.fr, zhanghj@pku.edu.cn; Funded by China Scholarship Council No. 2009601276 and by ANR project Multiple Impact ANR-08-BLAN-0321-01.

†INRIA, BIPOP project-team, ZIRST Montbonnot, 655 avenue de l'Europe, 38334 Saint Ismier, France, e-mail:Bernard.Brogliato@inrialpes.fr

‡State Key Laboratory for Turbulence and Complex Systems, College of Engineering, Peking University, Beijing 100871, People's Republic of China, e-mail: liucs@pku.edu.cn

asymmetry [10, 30], Coulomb friction outside the impacts [28, 33] or during the impacts with a kinematic restitution law [12], varying restitution coefficients [21], with compliance at the base [2], some kinds of "hybrid dynamical" models aiming at modeling the different possible modes taken by a block and the transitions between them [32], *etc.* One difficulty, that is overcome by the LZB impact model that is used in this paper (Part I and Part II), is to correctly model the effects of Coulomb friction within a rigid body approach, not only outside the impacts but also during the impacts. Even in the simplest case of single impact between two bodies this is known to be a hard task [6]. Usually Coulomb friction is modeled at the impulse level during the collisions and this is known to yield possible energetical inconsistency when coupled to Newton or Poisson's like restitution laws [4, 31]. This is avoided when energetical restitution laws are properly used.

The first part of this paper [38] focuses on the free-rocking motions, with fixed base. The second part is dedicated to the case with base excitation. As we shall show, free-rocking experiments may not be interesting *per se*, however they may well serve as parameter-fitting processes for the base-excitation simulations. In this Part II we consider that the ground is an excited base, with horizontal harmonic motion of the form $x_b(t) = \mathbf{A}\sin(\omega t)$, or a one-sine pulse type acceleration (see section 4.2). The block/ground system is depicted in figure 1.

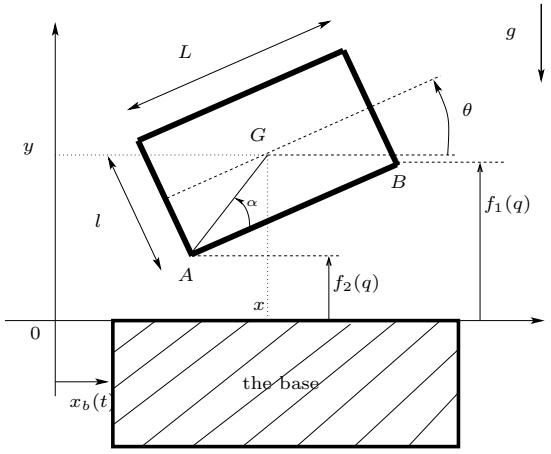

Figure 1: The planar block with horizontally moving base.

The dynamics is therefore given by (all the notations are the same as in Part I and are not recalled here):

$$\left\{\begin{array}{ll} m\ddot{x}(t) & = \lambda_{t,1}(t) + \lambda_{t,2}(t) \\ m\ddot{y}(t) & = \lambda_{n,1}(t) + \lambda_{n,2}(t) - mg \\ I_G\ddot{\theta}(t) & = \lambda_{n,1}(t)\left(\frac{l}{2}\sin(\theta(t)) + \frac{L}{2}\cos(\theta(t))\right) + \lambda_{n,2}(t)\left(\frac{l}{2}\sin(\theta(t)) - \frac{L}{2}\cos(\theta(t))\right) \\ & \quad + \left(\frac{l}{2}\cos(\theta) - \frac{L}{2}\sin(\theta)\right)\lambda_{t,1} + \left(\frac{l}{2}\cos(\theta) + \frac{L}{2}\sin(\theta)\right)\lambda_{t,2} \\ & \\ & 0 \le \lambda_n(t) \perp f(q(t)) \ge 0 \\ & \lambda_{t,i}(t) \in -\mu_i\lambda_{n,i}(t)\,\mathrm{sgn}(v_{t,i}(t) - v_b(t)), i = 1,2 \end{array}\right. \tag{1}$$

where $v_b(t) = \dot{x}_b(t)$ is the base horizontal velocity. It is assumed that the base has an infinite mass. One can rewrite (1) more compactly as follows:

$$\left\{\begin{array}{l} M\ddot{q}(t) = W_n(q(t))\lambda_n(t) + W_T(q(t))\lambda_t(t) - \mathbf{g} \\ \\ 0 \le \lambda_n(t) \perp f(q(t)) \ge 0 \\ \lambda_{t,i}(t) \in -\mu_i\lambda_{n,i}(t)\,\mathrm{sgn}(v_{t,i}(t) - v_b(t)), i = 1,2 \end{array}\right. \tag{2}$$

where the various terms are defined as $W_n(q) = \begin{pmatrix} 0 & 0 \\ 1 & 1 \\ \frac{l}{2}\sin(\theta) + \frac{L}{2}\cos(\theta) & \frac{l}{2}\sin(\theta) - \frac{L}{2}\cos(\theta) \end{pmatrix}$, $W_T(q) = \begin{pmatrix} 1 & 1 \\ 0 & 0 \\ \frac{l}{2}\cos(\theta) - \frac{L}{2}\sin(\theta) & \frac{l}{2}\cos(\theta) + \frac{L}{2}\sin(\theta) \end{pmatrix}$, $\lambda_n = (\lambda_{n,1}\ \lambda_{n,2})^T$, $\lambda_t = (\lambda_{t,1}\ \lambda_{t,2})^T$, $\mathbf{g} = (0\ mg\ 0)^T$. The sign function in (1) is the multivalued sign function, and is enhanced with static and dynamic friction (see figure 2 in Part I). The impact dynamics is the LZB model as in Part I (see section 2.2 in [38]), and the numerical code used to perform the simulations is identical: it is an event-driven algorithm that integrates (1) outside the impacts, with a suitable treatment of the complementarity conditions and of Coulomb friction (see [19] for details), and which computes the post-impact velocities with the LZB impact model each time a collision has been detected. This impact dynamics has been developed in [17, 18, 19, 20, 39] and allows one to model multiple impacts without or with Coulomb friction. The numerical code that is used in this paper is given in [37].

The paper is organized as follows: In section 2 we present a set of comparisons between numerical and experimental results, for rocking motion. Section 3 is dedicated to the study of the onset of rocking under harmonic horizontal base excitation. Section 4 presents some results about the onset of overturning, both with harmonic and one-sine pulse excitations. Conclusions end the paper in section 5. The flowcharts of the numerical code used in both Parts I and II are in section A.

2 Rocking motion: comparisons with experiments in [24]

Experiments with horizontal base excitation have been given in [24][1] for blue granite block/ground system. We consider here the specimen 2 in [24], see Part I for all details concerning this type of block. The base excitation has a harmonic the form $x_b(t) = \mathbf{A}\sin(\omega t)$. The parameters $e^*_{n,i}$ and μ, μ_s in the LZB model are those obtained from the free-rocking fitting process of Part I, *i.e.* $e^*_{n,i} = e^*_n = 0.999$, $\mu = 0.3$, $\mu_s = 0.577$, $l = 1$m, $L = 0.155$m. The free-rocking experiments may thus be considered as a simple process for parameter fitting. The results are reported in figure 2. It is seen that the LZB model has the tendancy to slightly underestimate the peaks magnitudes, however the frequency of the response is very well predicted. As shown in figure 12 in [24] through repeatability tests, the amplitude of the rocking angle $\theta(t)$ may vary from one experiment to the other, which may explain that the LZB model does not predict the same amplitude as in the experimental figures. We may anyway conclude that there is a very good matching between the numerical results and the experimental ones using the free-rocking fitted parameters of Part I.

Remark 1. *The DEM method employed for the simulations in [23] seems to provide comparable results to the LZB/complementarity one, see figure 7 in [23] that concerns specimen 2. As we already noted in Part I it is difficult at this stage of the studies to determine which of the two methods is the best one. It is however noteworthy that we have shown in Part I and this part, that the LZB/complementarity model and event-driven code, is able to correctly predict several types of motions (free-rocking, rocking with horizotal motion, onset of rocking) with three different sets of experimental results obtained by other authors. It is also recalled that the LZB model successfully predicted various motions of different impacting systems like chains of balls [18, 20] and bouncing dimer [39]. It therefore encaspulates the main dynamical effects which are necessary to well simulate multiple impacts for rate-independent materials, with parameters that possess a clear physical meaning for both the tangential and the normal dissipation effects.*

[1] We use here some data provided to us by Dr F. Pena from UNAM, Mexico.

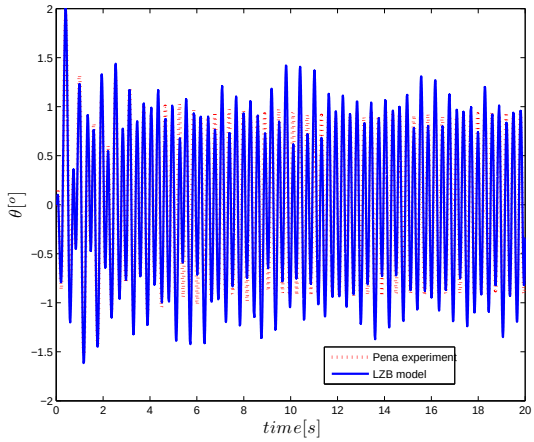

(a) Frequency $\frac{\omega}{2\pi}$ =3.3 hz, amplitude $\mathbf{A}$ =6 mm (specimen 1)

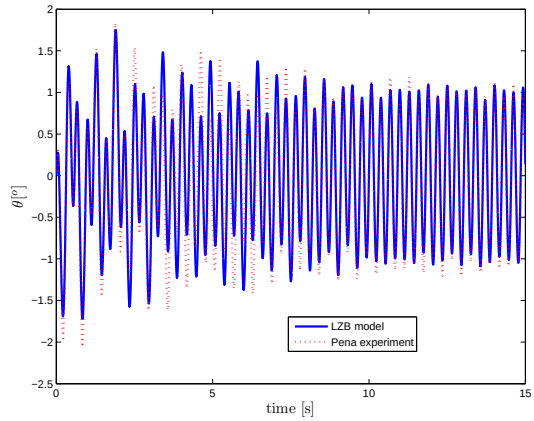

(b) Frequency $\frac{\omega}{2\pi}$ =3.3 hz, amplitude $\mathbf{A}$ =8 mm (specimen 2)

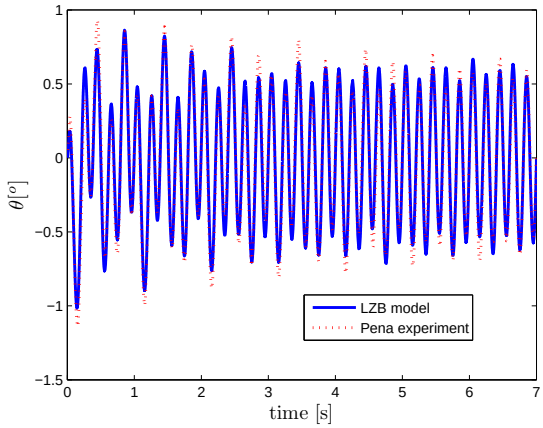

(c) Frequency $\frac{\omega}{2\pi}$ =3.3 hz, amplitude $\mathbf{A}$ =5 mm (specimen 2)

Figure 2: $\theta(t)$ responses with base excitation.

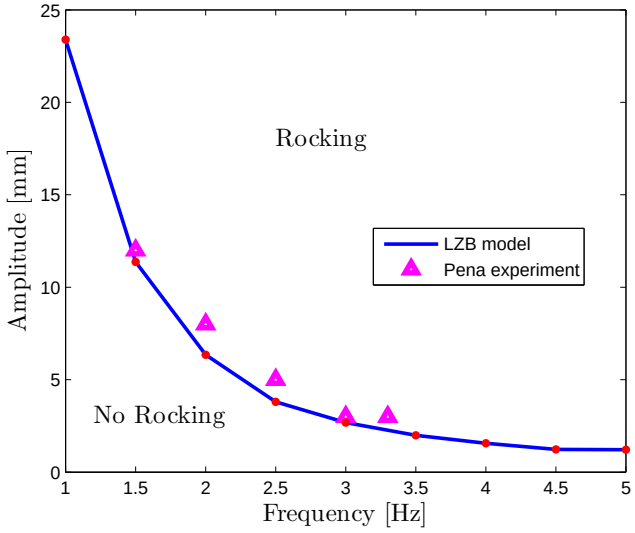

Figure 3: Onset of rocking for specimen 2.

3 Study of the onset of rocking

To start with the onset of rocking motion in the $(\mathbf{A}, \omega)$ plane is depicted in figure 3 with the experimental data taken from Table 4 in [24]. They concern specimen 2 with $l = 1$m, $L = 0.155$m, $d = 0.502$m, $m = 228$ kg. In all of this section $e^*_{n,i} = 0.99$. A good matching is found between the numerical and the experimental results. Notice that it is considered that rocking is initiated if the block not only starts to rock on the base, but if this rocking motion is persistent in time (*i.e.* the mere detachment of one contact point is not sufficient to decide for rocking). The tendency is that rocking starts to occur for large $\mathbf{A}$ when ω is small, and for small $\mathbf{A}$ when ω is large. This tendency is also in agreement with the experimental data of figure 14 in [34].

Let us now consider figure 4, which depicts the onset of rocking as a function of the aspect ratio $\frac{l}{L}$ and the amplitude $\mathbf{A}$, for a fixed frequency $\frac{\omega}{2\pi}$ =3.3 Hz. The points on the curve represent the lower limit of the necessary $\mathbf{A}$ for onset of rocking, *i.e.* rocking occurs for magnitudes just larger. Flat blocks need a large $\mathbf{A}$ to rock, while slender blocks rock for small $\mathbf{A}$. This seems intuitively clear. In figures 5 and 6 are depicted the trajectories $\theta(t)$ and the relative tangential velocity $\dot{x}_{rel}(t)$ at the contact point A. It is noteworthy that there exists a transition between all-stick regimes (very slender blocks) and all-slip regimes (very flat blocks). From figures 5 and 6 one sees that the transition occurs around $\frac{l}{L} = 3$. For $\frac{l}{L} = 3$ the relative velocity is almost always non zero, while for $\frac{l}{L} = 3.5$ it is almost always zero.

The figure 7 depicts the onset of rocking for base amplitude $\mathbf{A} = 5$mm. The friction parameters are varied. For high enough friction the onset of rocking occurs almost independently of the friction, but depends mainly on the aspect ratio $\frac{l}{L}$, corroborating previous results [27, 34]. For small enough friction however, there exists a minimum aspect ratio $\frac{l}{L}$ under which the onset of rocking starts to depend a lot on friction. When the friction is high enough the contacts statuses are mostly stick, therefore the value μ does not count whereas μ_s plays a role. Some interesting figures are reported in Tables 1 and 2. The mass m depends on the block's dimension, and increases with increasing l. These figures show that the product Af^2 that determines the onset of rocking, varies very little for a given aspect ratio $\frac{l}{L}$. This is not surprizing since Af^2 is directly related to the maximal acceleration of the base. Therefore the onset of rocking for a given aspect ratio, depends

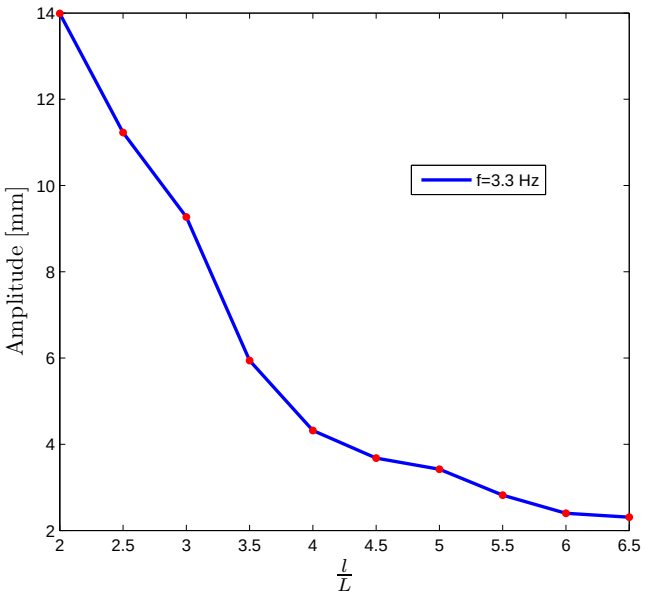

Figure 4: Onset of rocking, $L = 0.155$m, $\mu = 0.3$, $\mu_s = 0.577$.

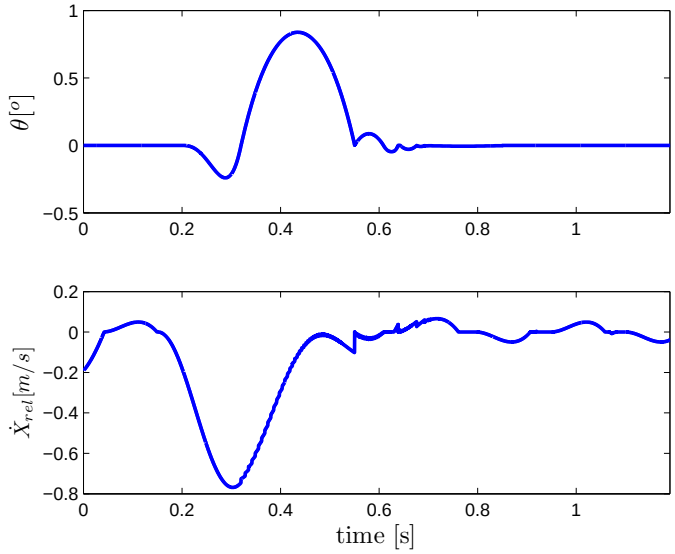

Figure 5: Responses $\theta(t)$ and relative tangential velocity, $\frac{l}{L} = 3$, $\mu = 0.3$, $\mu_s = 0.577$.

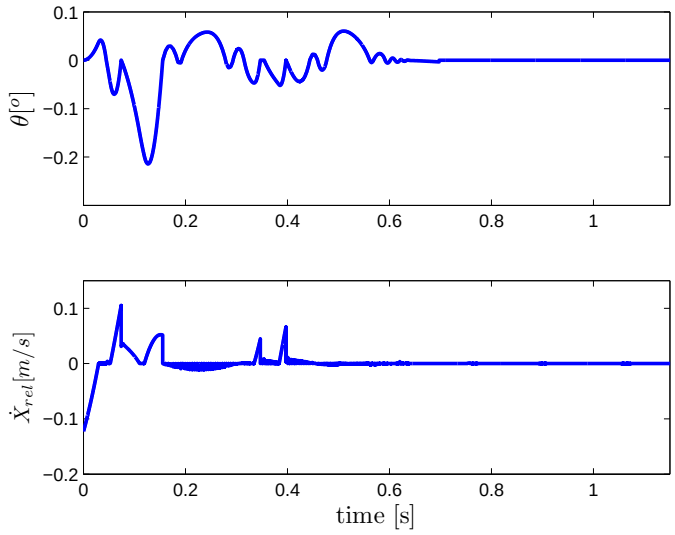

Figure 6: Responses $\theta(t)$ and relative tangential velocity, $\frac{l}{L} = 3.5$, $\mu = 0.3$, $\mu_s = 0.577$.

essentially on the maximal acceleration of the base. It is noteworthy that previous works report a criterion for the onset of rocking without sliding [14, 29, 25], which in fact reduces to a static equilibrium criterion $\mu_s \geq \frac{L}{l}$ (see *e.g.* equation (32) in [14]). The results obtained here do not make the sticking assumption, and some slipping phases are possible both outside and during the impacts. Clearly this changes a lot the onset of rocking conditions, in which the dynamical effects and the stick/slip transitions play a significant role. The maximal acceleration of the base is known to play a significant role in the block's dynamics, see *e.g.* [13] where this is denoted as PTA (for Peak Table Acceleration) and used to study the so-called Engineering Demand Parameter in purely sliding motions. It is also noteworthy that our results are not based on some model approximations as done sometimes [1] but keep the full non-linearity of the dynamics. The results for $\frac{l}{L} < 2$ are not depicted in figure 7. Indeed for such values of the aspect ratio and for realistic values of friction, the onset or rocking occurs for very large values of the frequency and one may infer that rocking never occurs.

4 Study of the overturning phenomenon

In this section the overturning phenomenon is studied numerically. Many studies have been devoted to the overturning phenomenon, see *e.g.* [1, 3, 10, 12, 13, 14, 15, 26, 28, 30, 32, 34]. In particular several works aim at defining simple enough criteria that may be used to assert if a block is likely to overturn or not. Our goal in this section is rather to prove that the LZB model may be useful to study the overturning because it encapsulates the rich dynamics of the block/ground system. Going further in the analysis is outside the scope of this work. Comparisons with existing numerical studies on the overturning are nevertheless presented.

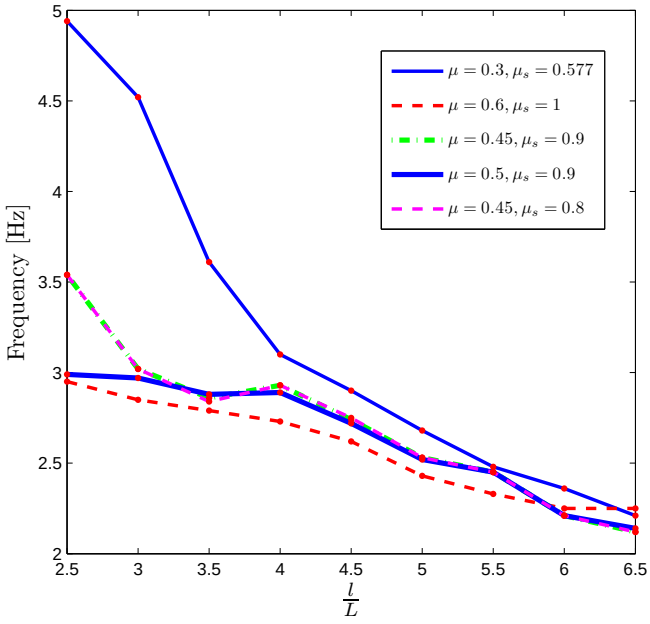

Figure 7: The onset of rocking with varying friction parameters.

$\frac{l}{L}$	2.0	2.5	3.0	3.5	4.0	4.5	5.0
f_1 ($A_1 = 3$mm)	7.08	6.51	5.91	4.68	4.05	3.71	3.49
A_2 ($f_2 = 3.3$Hz)	13.99	11.23	9.27	5.94	4.32	3.68	3.42
f_3 ($A_3 = 5$mm)	no rocking	4.94	4.52	3.61	3.10	2.90	2.68
f_4 ($A_4 = 7$mm)	no rocking	4.16	3.85	3.06	2.56	2.41	2.25
A_5 ($f_5 = 5.5$Hz)	no rocking	4.93	4.09	2.57	1.94	1.58	1.42
A_6 ($f_6 = 4$Hz)	no rocking	7.58	6.32	4.07	3.01	2.64	2.17
$A_1 f_1^2$	150.3792	127.1403	104.7843	65.7072	49.2075	41.2923	36.5403
$A_2 f_2^2$	152.3511	122.2947	100.9503	64.6866	47.0448	40.0752	37.2438
$A_3 f_3^2$	no rocking	122.0180	102.1520	65.1605	48.0500	42.0500	35.9120
$A_4 f_4^2$	no rocking	121.1392	103.7575	65.5452	45.8752	40.6567	35.4375
$A_5 f_5^2$	no rocking	123.25	102.25	64.25	48.5	39.5	35.5
$A_6 f_6^2$	no rocking	121.28	101.12	65.12	48.16	42.24	34.72

Table 1: The products Af^2 varying with $\frac{l}{L}$.

$\frac{l}{L}$	5.5	6.0	6.5
f_1 ($A_1 = 3$mm)	3.35	2.96	2.80
A_2 ($f_2 = 3.3$Hz)	2.82	2.40	2.31
f_3 ($A_3 = 5$mm)	2.48	2.36	2.21
f_4 ($A_4 = 7$mm)	2.07	1.90	1.83
A_5 ($f_5 = 5.5$Hz)	1.20	1.13	1.02
A_6 ($f_6 = 4$Hz)	1.86	1.66	1.53
$A_1 f_1^2$	33.6675	26.2848	23.5200
$A_2 f_2^2$	30.7098	26.1360	25.1559
$A_3 f_3^2$	30.7520	27.8480	24.4205
$A_4 f_4^2$	29.9943	25.27	23.4423
$A_5 f_5^2$	30	28.25	25.5
$A_6 f_6^2$	29.76	26.56	24.48

Table 2: The products Af^2 varying with $\frac{l}{L}$.

4.1 Harmonic base excitation

We first consider a horizontal harmonic motion of the base of the above form $x_b(t) = \mathbf{A}\sin(\omega t)$. It is expected that the overturning phenomenon hardly obeys simple rules, because it is known that the block's dynamics with moving base is an extremely sensitive process with respect to initial data and parameters, especially when restitution is high and stick/slip occurs [12]. In all the figures the curves are numbered starting with the smallest magnitude, or with the smallest frequency. The overturning is the result of an "optimal" exchange of energy between the base and the block, through an increase of the block's oscillation magnitude. This is illustrated in figure 8 (a), where the $\theta(t)$ response is depicted during 6s, with frequency $\frac{\omega}{2\pi} = 3.3$Hz, $e^*_{n,i} = 0.99$, $\frac{l}{L} = 6$ and $L = 0.155$m. This figure demonstrates that overturning may occur quickly for $\mathbf{A} = 40, 55, 60, 70, 30, 50$mm, later for $\mathbf{A} = 25, 35, 45, 65$mm, and not overturn for $\mathbf{A} = 15$mm before 6s. In all cases the block's motion before the overturn is quite similar in frequency and amplitude. This indicates that the overturn is the result of a sudden "break" in the base/block relative motion. Figure 8 (b) shows that decreasing $e^*_{n,i}$, *i.e.* adding normal dissipation at the impacts, decreases significantly the risk of overturning since all amplitudes $\mathbf{A} \leq 40$mm yield stable rocking. Figure 8 (c) shows that decreasing $\mathbf{A}$ may yield a stable rocking motion after some transient, as may be expected. In figure 9 the same study is done with varying frequencies and fixed $\mathbf{A} = 3$mm. Similar conclusions as for the varying amplitude can be drawn, that there is no monotonic variation of the overturning phenomenon as a function of the base frequency. Discontinuities in the dynamical behaviour are common in systems with impact and Coulomb friction. It is expected that more energy dissipation is going to prevent the block from overturning. Dissipation may come from two sources: sliding motions and normal restitution. The friction between the base and the block mainly influences the onset of rocking, for if $\mu = \mu_s = 0$ the block's corners never detach from the base. However when rocking has been established the most efficient way to "control" the overturning *via* energy dissipation is through the normal restitution, as demonstrated in figure 8 (b). Two comments are in order:

- In all the simulated cases of figures 8 and 9 there exist rebound phases after each impact at the corners. This means that the period of times with persistent contact between the ground and the block are very short or even vanish. Such bouncing phases tend to vanish when the slenderness increases (see Part I of this paper for the free-rocking case [38]).

- The base excitation is a persistent one. This means that it is difficult to assert firmly whether a motion is really stable or not, because the mechanism of energy transmission between the base and the block is very complex. For instance we cannot say if the motion with $\mathbf{A} = 40$mm in figure 8 (b) is stable or not on a long term. This is why studying overturning with simpler

base excitations like one sine period only may be useful.

4.2 Pulse-type base excitation

We now consider that the base has the pulse-type motion (called one-sine type-A pulse in [13, 22, 36]) with an acceleration equal to:

$$\dot{v}_b(t) = \begin{cases} a_p \sin(\omega_p t + \psi) & \text{if} \quad -\frac{\psi}{\omega_p} \leq t \leq \frac{2\pi - \psi}{\omega_p} \\ \\ 0 & \text{otherwise} \end{cases} \tag{3}$$

with $\psi = \arcsin(\frac{\alpha g}{a_p})$, $\alpha = \arctan(\frac{L}{l})$. The advantage of considering such base excitation is that it allows one to clearly separate the motions that overturn and those that do not overturn. Indeed once the base is at rest, the block may only lose energy. If it has not overturned before it starts to lose its energy, it will never overturn. This has been used in [13, 36], where one can find numerical results about the safe and unsafe areas depending on the amplitude and frequency of the base excitation (see for instance figure 6 in [13]). The results are reported in figures 10 to 14. The parameters are chosen as in [22, Figure 5], *i.e.* $l = 1.555$, $L = 0.3971$, $e_n^* = 0.9$, so that $p \triangleq \sqrt{\frac{3g}{4R}} = 2.14$ and $\alpha = \arctan(\frac{L}{l}) = 0.25$.

- In figure 10 are depicted various areas in the $(\frac{a_p}{\alpha g}, \frac{\omega_p}{p})$ plane. Qualitatively we recover the same shapes as in [13, Figure 6] or [22, Figures 5, 8, 9]: a big area (above the curve AGH or above the curve $AGJK$) within which overturning occurs with no impact, and a smaller "tongue shaped" area (within $AIDCB$ for $\mu = 0.3$, $\mu_s = 0.8$, different for the other two frictions) where overturning occurs after one or several impacts. There are however major discrepancies with respect to the results in [13, 22, 36]:
  - The models used in [13, 36] are of the Housner type, with basic assumptions like no slipping phases, and a constant angular velocity restitution r. The LZB model includes Coulomb friction and allows for stick/slip behaviour both outside and during the impacts, with a coherent energetical behaviour. Figures 11, 12, 13 (g) (h) (i) show that there is always an important slipping phase before the block overturns.
  - Consider the case $\mu = 0.5$, $\mu_s = 0.8$. The overturn in the area above the line AB and below the line AF, occurs after two impacts (which is new compared to [13, Figure 6] which indicates only one impact). There is a discontinuity between points B and C, because the overturning in the area above CD and below the next curve AFI occurs with one impact only.
  - The overturning area with one or two impacts, is larger than the one-impact overturning area in [13, Figure 6].
- As expected the safe area increases when the friction decreases, that indicates that more slip implies less overturn. In the frictionless limit there is no overturn since the block keeps slipping on the base.
- Figures 11 (a) (d) (g) correspond to a point on the line AB in figure 10, figures 11 (b) (e) (h) correspond to a point on the line CD, figures 11 (c) (f) (i) correspond to a point on the line AF. Figures 12 (a) (d) (g) correspond to a point on the line FE in figure 10, figures 12 (b) (e) (h) correspond to a point on the line AG, figures 12 (c) (f) (i) correspond to a point on the line FI. Figures 13 (a) (d) (g) correspond to a point on the line GJ in figure 10, figures 13 (b) (e) (h) correspond to a point on the line JI, figures 13 (c) (f) (i) correspond to a point in the right upper corner of figure 10.

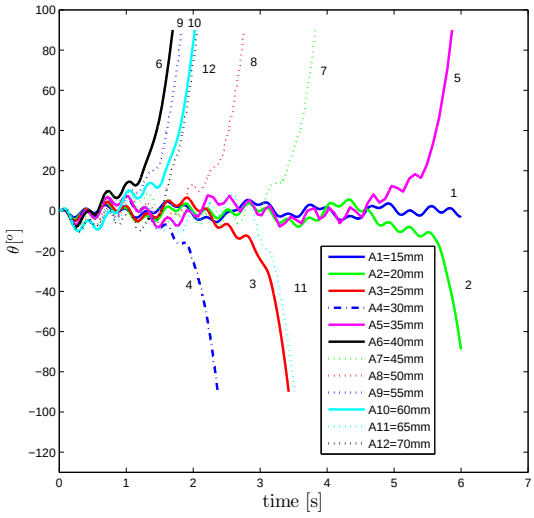

(a) Overturning amplitudes, $e^*_{n,i} = 0.99$.

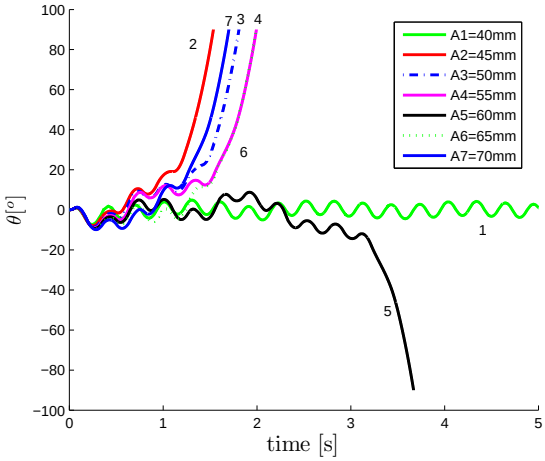

(b) Overturning amplitudes, $e^*_{n,i} = 0.8$.

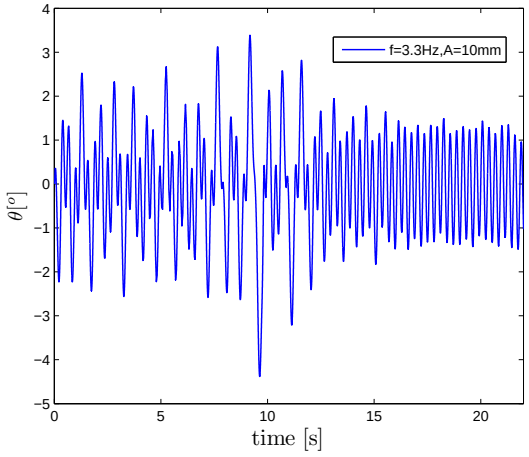

(c) Non-overturning amplitude.

Figure 8: The overturning with varying $\mathbf{A}$, $f = 3.3$Hz.

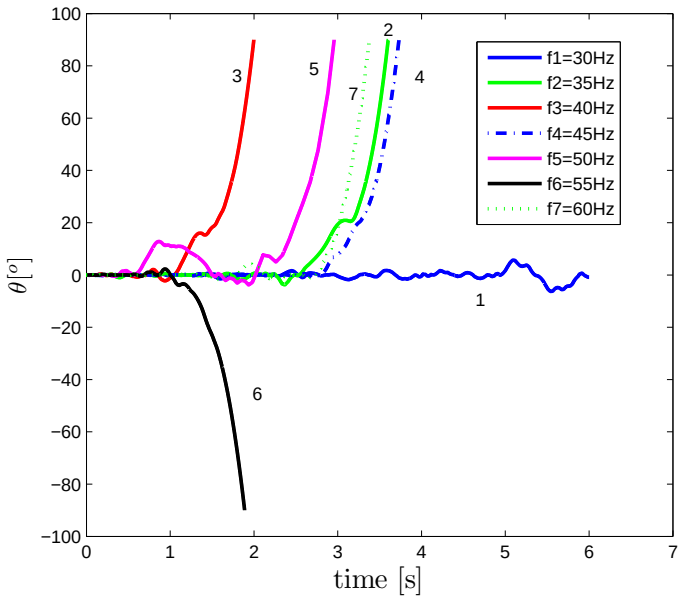

Figure 9: The overturning with varying ω, $\mathbf{A} = 3$mm.

- From figures 11, 12, 13 (g) (h) (i) one sees that the overturning is almost always occurring after a phase of slip, followed by a sticking phase at the point of contact (notice that the vertical scales in figures 11, 12, 13 (g) (h) (i) and in figures 11, 12, 13 (d) (e) (f) are quite different in magnitude).
- There are two impacts before the overturn in figure 11 (a). The first impact, however, has very small magnitude. In figure 14 (a) the first 0.3s of the simulation are zoomed, and the first impact can be seen when $\theta(t)$ crosses the zero value at $t \approx 0.15$s. In figure 14 (b) the first 0.5s of the $\theta(t)$ response of figure 11 (b) are shown and it is seen that there is only one impact at $t \approx 0.42$s before the overturn. Recall that these two cases correspond to points of the lines AB and CD respectively.

The overturning phenomenon is certainly the most complex phenomenon that may occur in the block/ground system. Our numerical results mainly aim at showing that the LZB model with friction, coupled to the complementarity system in (1) outside the impacts, may improve our knowledge about overturning in planar blocks. It is to be considered as a preliminary work because on the first hand three-dimensional effects are likely to play a significant role in most of the experiments with strong base excitation, on the second hand real earthquakes excitations are more complex than those considered here.

5 Conclusions

This second part presents some results on the onset of rocking and of overturning of planar blocks, when the base is subject to harmonic or one-sine pulse excitations. Comparisons for the rocking and the onset of rocking are made with available experimental data, showing quite good agreement. For the overturning phenomena only numerical simulations are presented. The impact model that is used allows one to correctly handle multiple impacts with friction and has been validated on

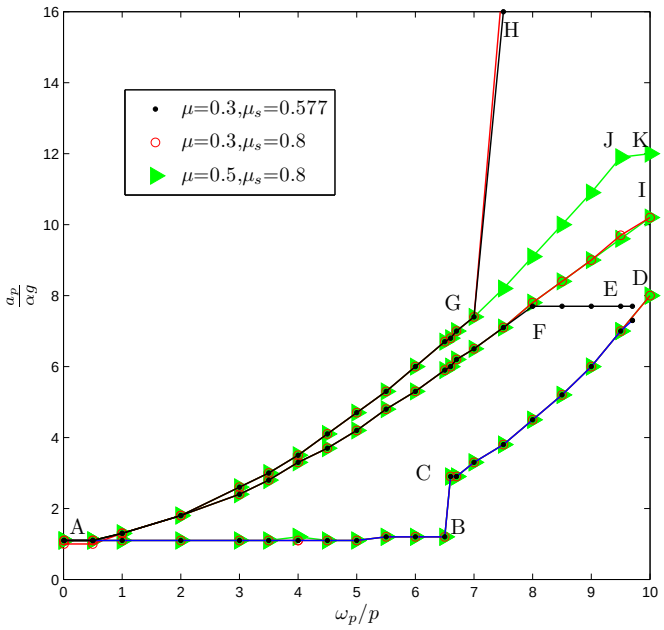

Figure 10: Overturning safe and unsafe areas.

different types of mechanical systems with impacts and friction in previous papers [17, 18, 19, 20, 39]. The results of Parts I and II show that this impact model encapsulates the main features of the block/ground system, and most importantly allows one to take stick/slip behaviours into account, both outside and during the impacts. They pave the way towards future studies that should focus on a three-dimensional model (with four contact points), more sophisticated base excitations, and the incorporation of flexibilities in the structure.

Ackowledgements: the authors are very grateful to Dr Fernando Pena (UNAM Mexico) for providing them with detailed figures from the experiments in [24]. These data have been valuable for achieving this work. This work was performed with the support of the NSFC/ANR project Multiple Impact, ANR-08-BLAN-0321-01.

A The flowcharts of the event-driven method

See figures 15 and 16.

References

[1] H. Al Abadi, N. Lam, E. Gad, "A simple displacement-based model for predicting seismically induced overturning", Journal of Earthquake Engineering, vol.10, no 6, pp.775-814, 2006.

[2] U. Andreaus, P. Casini, "Dynamics of three-block assemblies with unilateral deformable contacts. Part 1: contact modelling", Earthquake Engineering and Structural Dynamics, vol.28, pp.1621-1636, 1999.

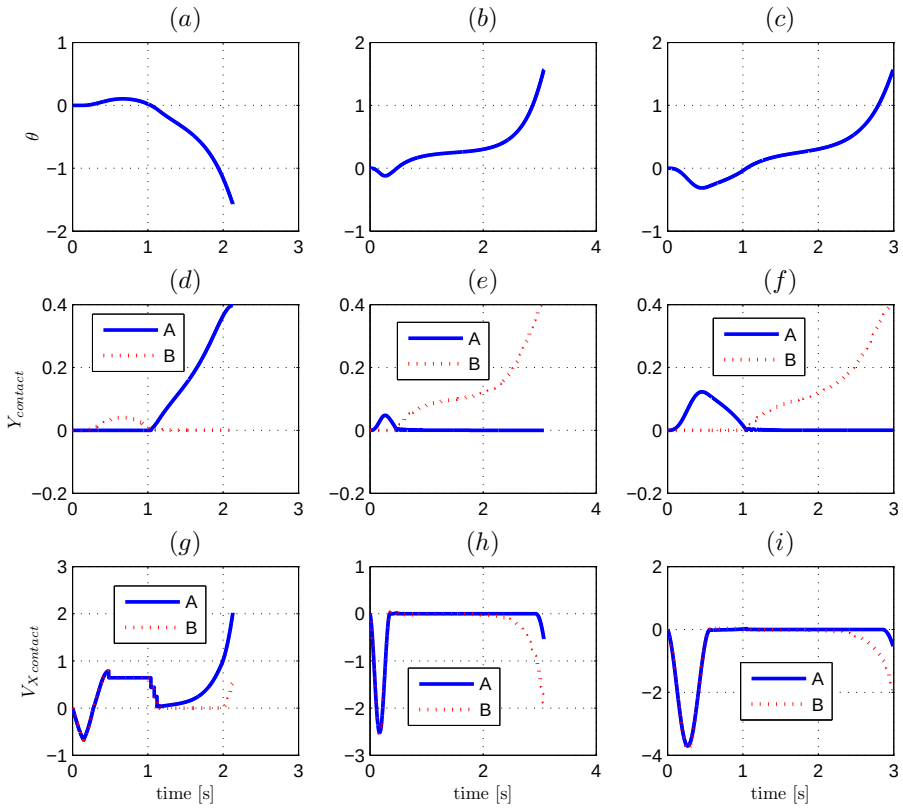

Figure 11: (a) (b) (c): $\theta(t)$, (d) (e) (f) vertical positions and (g) (h) (i) relative horizontal velocities of the contact points.

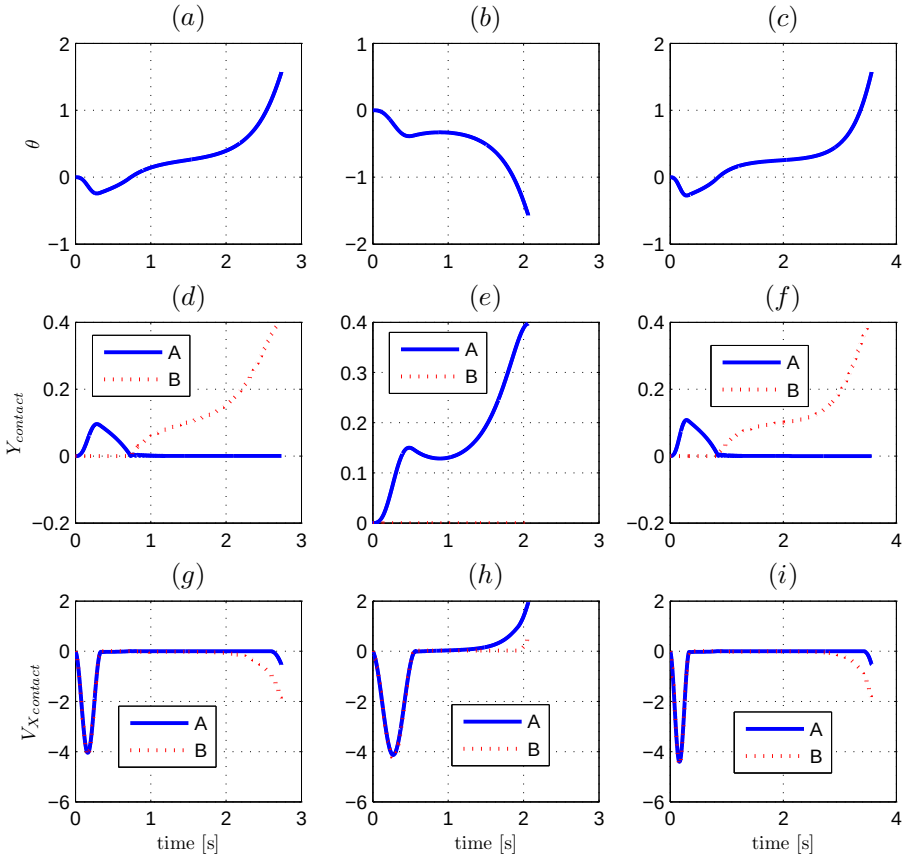

Figure 12: (a) (b) (c): $\theta(t)$, (d) (e) (f) vertical positions and (g) (h) (i) relative horizontal velocities of the contact points..

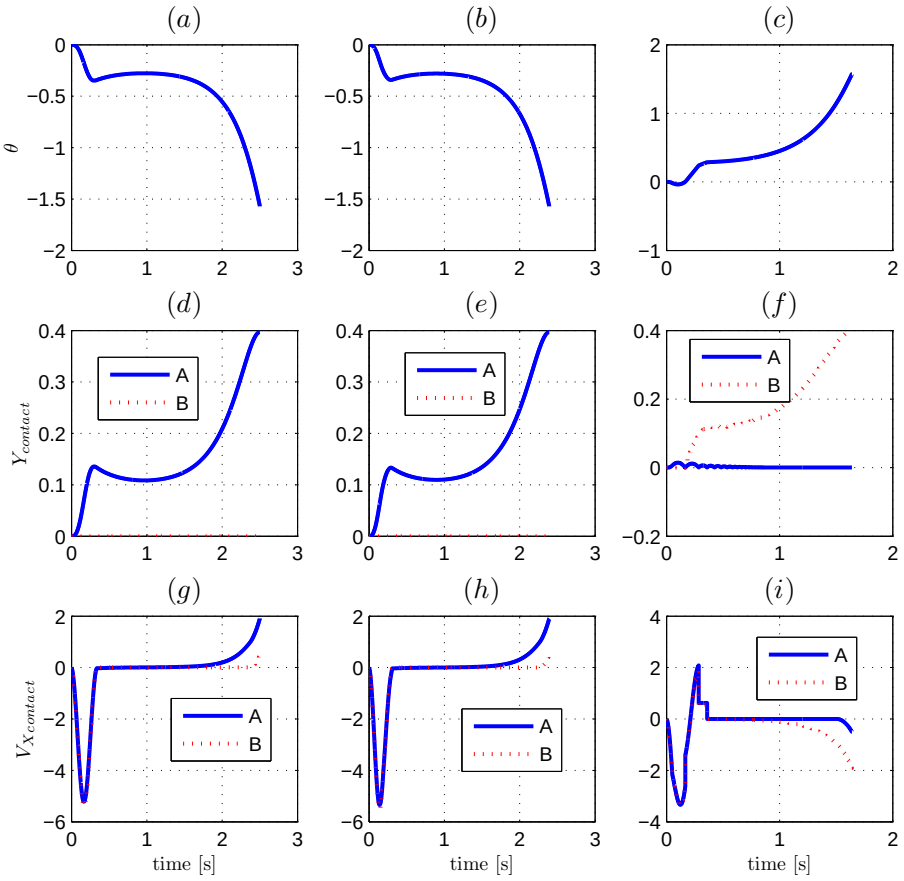

Figure 13: (a) (b) (c): $\theta(t)$, (d) (e) (f) vertical positions and (g) (h) (i) relative horizontal velocities of the contact points..

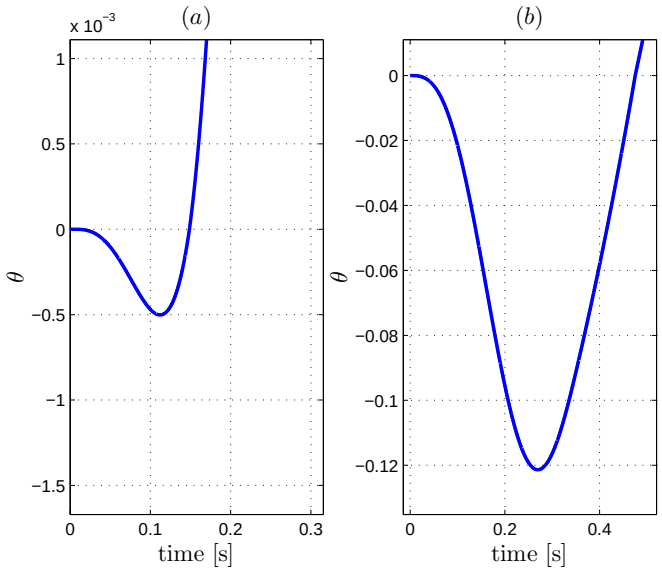

Figure 14: Zooms of figures 11 (a) and (b).

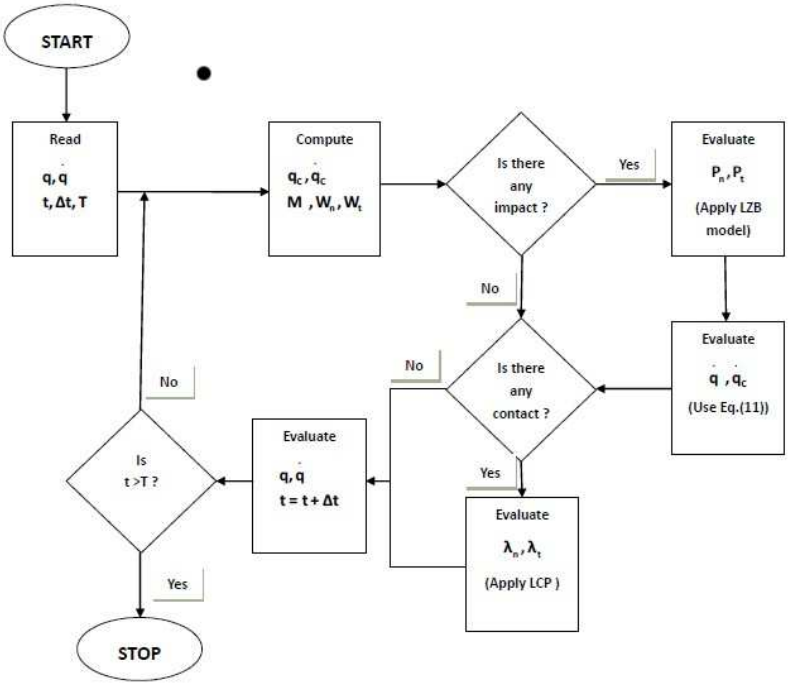

Figure 15: General flowchart of the event-driven code.

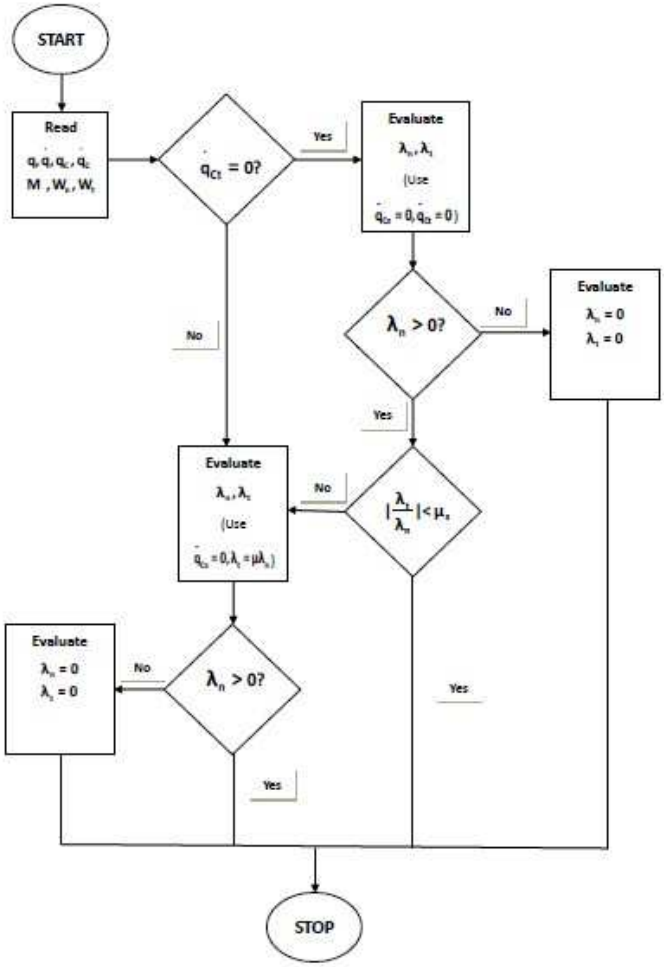

Figure 16: Flowchart for the calculation of the contact/impact forces.

[3] R. Boroschek, A. Iruretagoyena, "Controlled overturning of unanchored rigid bodies", Earthquake Engineering and Structural Dynamics, vol.35, no 6, pp.695-711, 2006.

[4] B. Brogliato, *Nonsmooth Mechanics*, Springer London, 2nd Ed., 1999.

[5] B. Brogliato, H. Zhang, C. Liu, "The planar rocking-block: analysis of a generalized kinematic restitution law", submitted.

[6] S. Djerassi, "Collision with friction; Part A: Newton's hypothesis", Multibody Systems Dynamics, vol.29, pp.37-54, 2009.

[7] S. Dorbolo, D. Volfson, L. Tsimring, A. Kudrolli, "Dynamics of a bouncing dimer", Physical Review Letters, vol.95, no 4, art. no 044101, pp. 1-4, 2005.

[8] A. Di Egidio, A. Contento, "Base isolation of slide-rocking non-symmetric rigid blocks under impulsive and seismic excitations", Engineering Structures, vol.31, pp.2723-2734, 2009.

[9] M.A. ElGawady, Q. Ma, J. W. Butterworth, J. Ingham, "Effects of interface material on the performance of free rocking blocks", Earthquake Engineering and Structural Dynamics, vol.40, no 4, pp.375-392, April 2011..

[10] W.T. Fielder, L.N. Virgin, R.H. Plaut, "Experiments and simulation of overturning of an asymmetric rocking block on an oscillating foundation", European Journal of Mechanics A/Solids, vol.16, no 5, pp.905-923, 1997.

[11] G.W. Housner, "The behaviour of inverted pendulum structures during earthquakes", Bulletin of the Seismological Society of America, vol.53, no 2, pp.403-417, 1963.

[12] M.Y. Jeong, K. Suzuki, S.C.S. Yim, "Chaotic rocking behavior of freestanding objects with sliding motion", Journal of Sound and Vibration, vol.262, pp.1091-1112, 2003.

[13] D. Konstantinidis, N. Makris, "Experimental and analytical studies on the responses of 1/4-scale models of freestanding laboratory equipment subjected to strong earthquake shaking", Bulletin Earthquake Engineering, vol.8, pp.1457-1477, 2010.

[14] A.N. Kounadis, "On the overturning instability of a rectangular rigid block under ground excitation", The Open Mechanics Journal, vol.4, pp.43-57, 2010.

[15] S. Lenci, G. Rega, "A dynamical systems approach to the overturning of rocking block", Chaos, Solitons and Fractals, vol.28, no 2, pp.527-542, 2006.

[16] P.R. Lipscombe, S. Pellegrino, "Free rocking of prismatic blocks", Journal of Engineering Mechanics, vol.119, no 7, pp.1387-1410, July 1993.

[17] C. Liu, Z. Zhao, B. Brogliato, 2008 "Frictionless multiple impacts in multibody systems: Part I. Theoretical framework", Proceedings of the Royal Society A, Mathematical, Physical and Engineering Sciences, vol.464, no 2100, pp.3193-3211, December.

[18] C. Liu, Z. Zhao, B. Brogliato, 2008 "Energy dissipation and dispersion effects in a granular media", Physical Review E, vol.78, no 3, 031307, September.

[19] C. Liu, Z. Zhao, B. Brogliato, 2008 "Variable structure dynamics in a bouncing dimer", INRIA Research Report 6718, November, http://hal.inria.fr/inria-00337482/fr/ .

[20] C. Liu, Z. Zhao, B. Brogliato, 2009 "Frictionless multiple impacts in multibody systems: Part II. Numerical algorithm and simulation results", Proceedings of the Royal Society A, Mathematical, Physical and Engineering Sciences, vol.465, no 2101, pp.1-23, January.

[21] Q.T.M. Ma, *The Mechanics of Rocking Structures subjected to Gournd Motion*, PhD thesis, Department of Civil and Environmental Engineering, The University of Auckland, New Zealand, July 2010.

[22] N. Makris, J. Zhang, "Rocking response and overturning of anchored equipment under seismic excitations", PEER Report 1999/06, Pacific Earthquake Engineering Research Center, College of Engineering, University of California, Berkeley, November 1999, available at http://nisee.berkeley.edu/elibrary/Text/1200242 .

[23] F. Pena, F. Prieto, P.B. Lourenço, A. Campos Costa, J.V. Lemos, "On the dynamics of rocking motion of single rigid-block structures", Earthquake Engineering and Structural Dynamics, vol.36, pp.2383-2399, 2007.

[24] F. Pena, P.B. Lourenço, A. Campos-Costa, "Experimental dynamic behavior of free-standing multi-block structures under seismic loadings", Journal of Earthquake Engineering, vol.12, pp.953-979, 2008.

[25] A. Pompei, A. Scalia, M.A. Sumbatyan, "Dynamics of rigid block due to horizontal gorund motion", J. Eng. Mech. ASCE, vol.124, no 7, pp.713-717, 1998.

[26] M.D. Purvance, A. Anooshehpoor, J.N. Brune, "Freestanding block overturning fragilities: Numerical simulation and experimental validation", Earthquake Engineering and Structural Dynamics, vol.37, pp.791-808, 2008.

[27] M. Raous, "Experimental analysis of the rocking of a rigid block", 3rd Pan American Congress of Applied Mechanics (PACAM III), Sao Paolo, Brazil, Jaunary 4-8 1993.

[28] Y. Shao, C.C. Tung, "Seismic response of temporary structures", Nuclear Engineering and Design, vol.181, pp.267-274, 1998.

[29] H.W. Shenton, "Criteria for initiation of slide, rock, and slide-rock rigid-body modes", J. Eng. Mech. ASCE, vol.122, no 7, pp.690-693, 1996.

[30] B. Shi, A. Anooshenhpoor, Y. Zeng, J.N. Brune, "Rocking and overturning of precariously balanced rocks by earthquakes", Bulletin of the Seismological Society of America, vol.86, no 5, pp.1364-1371, October 1996.

[31] W.J. Stronge, *Impact Mechanics*, Cambridge University Press, 2000.

[32] T. Taniguchi, "Non-linear response analyses of rectangular rigid bodies subjected to horizontal and vertical ground motion", Earthquake Engineering and Structural Dynamics, vol.31, pp;1481-1500, 2002.

[33] T. Taniguchi, "Experimental and analytical study of free lift-off motion induced slip behavior of rectangular rigid bodies", ASME Journal of Pressure Vessel technology, vol.126, pp.53-58, February 2004.

[34] T. Winkler, K. Meguro, F. Yamazaki, "Response of rigid body assemblies to dynamic excitation", Earthquake Engineering and Structural Dynamics, vol.24, pp.1389-1408, 1995.

[35] C. Yilmaz, M. Gharib, Y. Hurmuzlu, "Solving frictionless rocking block problem with multiple impacts", Proc. R. Soc. A, vol.465, pp.3323–3339, 2009.

[36] J. Zhang, N. Makris, "Rocking response of anchored blocks under pulse-type motions", Journal of Engineering Mechanics, vol.127, no 5, pp.411-529, 2001.

[37] H. Zhang, B. Brogliato, "The planar rocking block: analysis of kinematic restitution laws, and a new rigid-body impact model with friction", INRIA Research Report RR-7580, March 2011, http://hal.inria.fr/inria-00579231/en/.

[38] H. Zhang, B. Brogliato, C. Liu, "Comparisons between numerical and experimental data for the planar rocking-block dynamics– Part I: free-rocking", submitted.

[39] Z. Zhao, C. Liu, B. Brogliato, 2009 "Planar dynamics of a rigid body system with frictional impacts. II. Qualitative analysis and numerical simulations", Proceedings of the Royal Society A, Mathematical, Physical and Engineering Sciences, vol.465, no 2107, pp. 2267-2292, July.